# Energy relaxation for hot Dirac fermions in graphene and breakdown of the quantum Hall effect

A. M. R. Baker, J. A. Alexander-Webber, T. Altebaeumer, and R. J. Nicholas*
*Department of Physics, University of Oxford, Clarendon Laboratory, Parks Road, Oxford, OX1 3PU, United Kingdom*
(Received 18 November 2011; revised manuscript received 26 January 2012; published 5 March 2012)

Energy loss rates for hot carriers in graphene are experimentally investigated by observing the amplitude of Shubnikov-de Haas oscillations as a function of electric field. The carrier energy loss in graphene follows the predictions of deformation potential coupling going as $\sim T^4$ at carrier temperatures up to $\sim$100 K, and that deformation potential theory, when modified with a limiting phonon relaxation time, is valid up to several hundred Kelvin. Additionally we investigate the breakdown of the quantum Hall effect and show that energy loss rates in graphene are around ten times larger than GaAs at low temperatures. This leads to significantly higher breakdown currents per micrometer, and we report a measured breakdown current of 8 $\mu$A/$\mu$m.

DOI: 10.1103/PhysRevB.85.115403 PACS number(s): 72.80.Vp, 73.43.−f

## I. INTRODUCTION

Graphene has been hailed in the few years since its discovery as the ideal material for a range of applications from gas sensors to touch screens. This is in large part due to its unusual properties, many of which are ultimately derived from its unique linear electronic dispersion relation. One of the most exciting potential uses for graphene is as a successor to silicon for microchip manufacture. Indeed the semiconductor industry roadamp[1] lists graphene as a leading candidate to replace silicon in nanoelectronics. For such a use it has many favorable properties, including an ultrahigh room temperature mobility[2] of $>$10,000 cm$^2$/(V s), its ability to integrate to nearly any substrate,[3] the stability of its carbon-carbon bond, its single atom thickness which should allow for greater gate length scalability according to scaling theory,[4] and the fact that it is amenable to conventional planar processing techniques.

As the size of electronics goes down the power density increases, and as a result heat management is now a primary constraint in operating performance. It is therefore of great practical as well as theoretical interest to understand how energy is lost from the carriers in graphene to its lattice. There have been a number of theoretical calculations of the energy loss rate per carrier,[5,6] but to date there have only been limited experimental results reported. In this paper we report measurements of the energy loss per carrier in the regime of total energy loss $\sim$1–500 W cm$^{-2}$, comparable to that found in modern central processor units.

The large value of the cyclotron energy $\hbar\omega_c$ for graphene also means that the beginnings of quantum Hall behavior can be observed at room temperature,[2] leading to suggestions that it would be a good material for quantum Hall resistance standards applications. Results to date on exfoliated graphene have not reported particularly high breakdown currents,[7] whereas by contrast reports on epitaxial graphene[8,9] suggest breakdown currents may be much higher than those for GaAs.[10] We demonstrate here that high breakdown currents can be observed for exfoliated graphene, and we relate these to the energy loss rates.

Our measurements of carrier heat loss have been taken in an intermediate temperature regime using magnetotransport measurements with carrier temperatures from 1.5 K to around 120 K. Most previous experimental work on energy loss rates in graphene has been done using optical excitation at much higher energies[11,12] with nonequilibrium carrier distributions and carrier temperatures in excess of 5000 K. In this regime the carrier lifetime has saturated, whereas we are able to show a significant dependence on temperature of the energy loss rate. Previous electrical studies have also concentrated on much higher temperature regimes, up to 1050 K.[13]

One reason for the considerable advantages of graphene over other materials is that polar-optical phonon scattering and piezoelectric acoustic phonon scattering are negligible up to room temperature and beyond due to the high optic phonon energy and nonionic bonding. At room temperature, deformation potential induced electron-acoustic phonon coupling is the only significant intrinsic scattering mechanism in contrast to most other semiconductors, where electron-optical phonon coupling is dominant. In all but the cleanest suspended samples however, scattering from substrate phonons and charged impurity scattering will tend to dominate,[14] with the high mobilities observed at room temperature[2] being observable only in ultraclean samples, and the ultrahigh mobilities only in suspended samples.[15] This might lead one to expect that electron energy loss rates in graphene would be rather small, however we demonstrate here that this is not the case, in agreement with theoretical predictions from Kubakaddi.[5] One consequence of this is that graphene has considerable potential for quantum Hall resistance standards capable of operating at high current densities.

## II. METHODOLOGY

### A. Sample preparation

The graphene was produced by the now standard micromechanical exfoliation technique[16,17] onto a silicon wafer with a 300 nm $SiO_2$ layer. The wafer was then diced into chips. Bond-pads and alignment marks were written using e-beam lithography and metal evaporation with a 20 nm adhesion layer of chrome and 200 nm of gold. The position of monolayer flakes were identified using the alignment marks, and hence the final fingers to the flake were written in a similar manner. Crucially, however, the final fingers were made by deposition of only gold without a chrome adhesion layer, as preliminary work showed that this gold-only contacting dramatically reduced the contact resistances to our devices. Our ungated Hall-bar devices were deliberately not mesa-etched giving

 

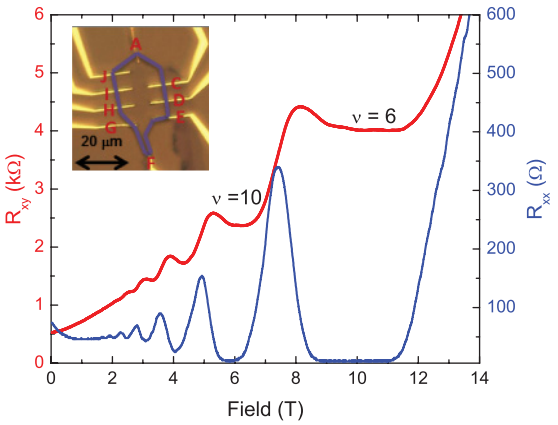


FIG. 1. (Color online) Example $R_{xx}$ and $R_{xy}$ quantum Hall effect traces from our device. The inset to the figure shows the layout of our device, and the outline of the monolayer graphene sheet is highlighted, clearly showing all gold contacts reaching inside the flake in an internal contacting geometry. The traces in this figure were taken in a nonstandard transverse geometry with the current running from D to H. The clear, adjacent $\nu = 6$, 10 plateaux demonstrate our sample to be monolayer graphene.

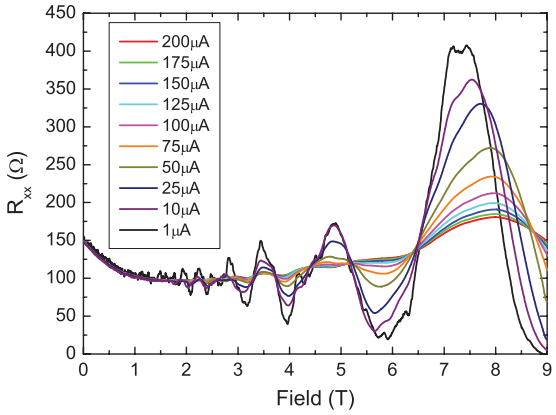


FIG. 2. (Color online) $R_{xx}$ measurements taken for a range of currents from 1 to 200 $\mu$A. Damping of the Shubnikov-de Haas oscillations are clearly observed. This data was again taken in a nonstandard geometry, this time with the current across the width of the sample between C and I.

a nonstandard internal contacting geometry. This was done in order to reduce the role of defects from edge states, by physically separating the currents from flowing near the edge of the device, and by minimizing the role of defect states and doping introduced by the mesa-etching process.[18] The device used in our experiments was connected in a standard Hall-bar arrangement (inset to Fig. 1).

### B. Measurement and data processing

Electrical measurements were carried out using a helium cooled 21 T Oxford Instruments magnet. We used a Kiethley SMU to supply current to the Hall-bar. All electrical measurements were made using Keithley 2000 DMMs. The samples were immersed directly in liquid helium at 1.5 K throughout. The area in which current flows is assumed to be internal to the area defined by the gold contacts, which have a much lower resistance than the graphene. When the applied current was passed along the length of the device, we took the relevant area to be the whole of the device inside the contacts. Most of our data was, however, collected in an alternative geometry, with the current passed across the width of the device. In this case simple Laplace equation modeling,[19] taking the current contacts as point contacts inside a uniformly conducting system, showed that the area of current flow is approximately circular with a diameter equal to the distance between the two current contacts.

## III. RESULTS

### A. Energy loss rate

We investigate carrier energy loss to the lattice by measuring the Shubnikov-de Haas oscillations and analyzing the damping of these oscillations to determine the carrier temperature, as has been reported previously in a number of different materials.[10,20–23] This is based on the assumption that there is a very rapid thermalization of the carriers which takes place on a time scale of tens of femtoseconds, leaving a Bolzmann distribution of hot carriers which then lose energy to the lattice much more slowly. Experiments in graphene and related materials strongly support this assumption of very rapid carrier thermalization.[11,12,24]

At low dc and ac currents, we observe typical well resolved quantum Hall behavior (Fig. 1) with $\nu = 6$ and $\nu = 10$ plateaux well defined in $R_{xy}$, with the associated $R_{xx}$ at zero resistance to within our measurement accuracy. The plateaux numbers observed follow the $2 + 4n$ pattern which confirms that our sample is monolayer graphene.[25] A series of measurements at constant dc currents ranging from 1 to 200 $\mu$A are shown in Fig. 2. As the current increases, the amplitude of the oscillations decreases, due to the increased carrier temperature from current heating. Using the theory of Ando[26] we calculate the carrier temperatures ($T_e$) from

$$\frac{\Delta\rho}{\rho} = f(\omega_c\tau)\frac{\chi}{\sinh\chi}e^{-\frac{\pi}{\omega_c\tau_s}}, \tag{1}$$

where

$$\chi = \frac{2\pi^2 k_B T_e}{\hbar\omega_c}, \tag{2}$$

and $\hbar\omega_c$ is calculated from the Landau level separations from

$$E_N = \mathrm{sgn(N)} \times c^*\sqrt{2e\hbar B|N|}, \tag{3}$$

where $|N|$ is the Landau quantum index and $B$ is the magnetic field. The Dirac velocity, $c^*$,[2,27] is taken to be $1.1 \times 10^6$ ms$^{-1}$. We estimate that our calculated values for $T_e$ have an associated random error of approximately 3–5%, with the error increasing at larger currents due to the smaller measured amplitudes.

Figure 3 shows a plot of $T_e$ as a function of current for the two plateaux. All measurements give electron temperatures in the range 20–120 K, demonstrating that we are operating in the nonequilibrium hot carrier regime. From this data we calculate the energy loss per carrier, taking into account that for short channel devices, the dominant power input is at the current

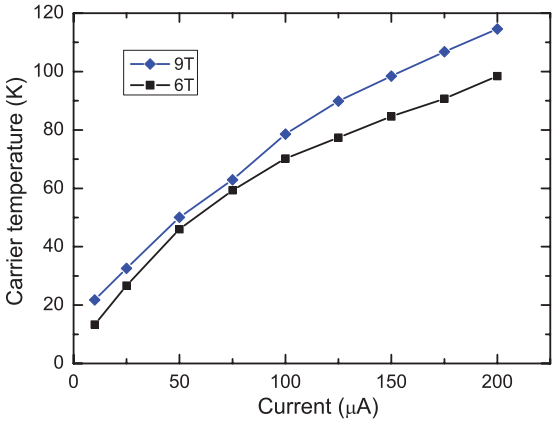


FIG. 3. (Color online) Measured carrier temperature as a function of input current for $\nu = 6,10$. Note the temperature attained is far in excess of that of the lattice which was held at 1.5 K throughout, and hence are operating in a hot carrier regime.

injecting contacts[28] where the voltage drop corresponds to the quantum Hall resistance $R_K$ using

$$E_{\text{loss}} = \frac{I^2 \frac{R_K}{\nu}}{N_e A}, \tag{4}$$

where we have used the measured charge carrier density of $N_e = 1.39 \times 10^{12}$ cm$^{-2}$ and device area as $A = 5.9 \times 10^{-11}$ m$^2$.

Combining this with the carrier temperature data gives the energy loss rate per carrier as a function of carrier temperature (Fig. 4). As found in other systems at low temperatures,[10,20–23,29,30] this shows an approximate power law dependence $\sim T^3 - T^4$. Theoretical predictions for energy loss rates are shown from the work of Kubakaddi[5]

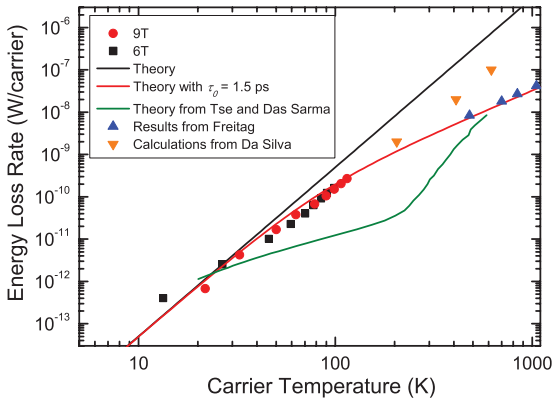


FIG. 4. (Color online) Carrier energy loss rate as a function of carrier temperature. Data from two plateaux are shown for 9 T and 6 T corresponding to $\nu = 6,10$ respectively. Superimposed in black is the unmodified theoretical prediction from Kubakaddi.[5] The red theory line is the prediction from Kubakaddi modified with the addition of a constant phonon relaxation time of 1 ps. The green theory line is a prediction from Tse and Das Sarma.[6] Finally some high lattice temperature data from Freitag[13] and calculations including silicon dioxide substrate phonons from Da Silva[31] are included.

for acoustic phonons, extrapolated from low-temperature values as

$$P = \alpha\left(T_e^4 - T_L^4\right), \tag{5}$$

where $\alpha$ is weakly carrier density dependent. Also shown are the theoretical predictions from Tse and Das Sarma.[6] These suggest a significantly lower contribution from acoustic phonons, with high-temperature energy loss, above ~250 K, being dominated by optical phonons. We find the Tse and Das Sarma prediction to fit our data poorly, significantly underestimating the energy loss rate for the majority of our measured range. Additionally the predicted power dependence of the range dominated by acoustic phonons is $\sim T^2$, which is lower than typically seen in other systems.[10,20–23,29,30] It is clear that the Kubakaddi acoustic phonon prediction,[5] based on a deformation potential of 19 eV, fits very well at lower temperatures, but the extrapolation increasingly overstates the measured values at higher carrier temperatures. Kubakaddi suggests that the theory requires extension[5] to provide accurate predictions in this range. The electron energy loss time ($\tau_e$) can be deduced from $P$ using

$$\tau_e = \frac{\pi^2 k_B^2 \left(T_e^2 - T_L^2\right)}{3 E_F P}, \tag{6}$$

where $T_L$ is the lattice temperature. This gives

$$\tau_e = \frac{\pi^2 k_B^2}{3 E_F \alpha T_e^2}, \tag{7}$$

when high $T_e \gg T_L$. At high temperatures $\tau_e$ is expected to saturate due to hot phonon and higher order effects. This has been measured optically for high energies both for doped and undoped samples.[11,12,24,32] For doped samples comparable to that studied here, the relaxation time has been measured to be in the range of 0.4–1.5 ps. Adding $\tau_0$ as a limiting factor we expect

$$\tau_e = \frac{\pi^2 k_B^2}{3 E_F \alpha T_e^2} + \tau_0. \tag{8}$$

In our modeling we have selected a value of 1 ps for the phonon relaxation time, which is in the middle of the measured range of values for doped graphene. We use this expression to recalculate $P$ from Eq. (6), giving

$$P = \frac{\pi^2 k_B^2 \alpha T_e^4}{\pi^2 k_B^2 + 3 E_F \alpha T_e^2 \tau_0}. \tag{9}$$

This expression gives good agreement with experiment for the whole temperature range, as shown in red in Fig. 4. In the figure we also include measurements from Freitag[13] of lattice temperature, a lower bound on the carrier temperature, at very high electron energy loss rates,[13] and calculations for electron temperatures including the silicon dioxide substrate phonons.[31] These suggest that the deformation potential scattering is still making a substantial contribution to energy loss rates up to temperatures of many hundreds of Kelvin and that Eq. (9) provides a good empirical description of the total energy loss rate.

The electron temperature dependence of $\tau_e$ is shown in Fig. 5, as deduced from experiment and Eq. (6), together with corresponding data for GaAs.[33] This shows the initially rather

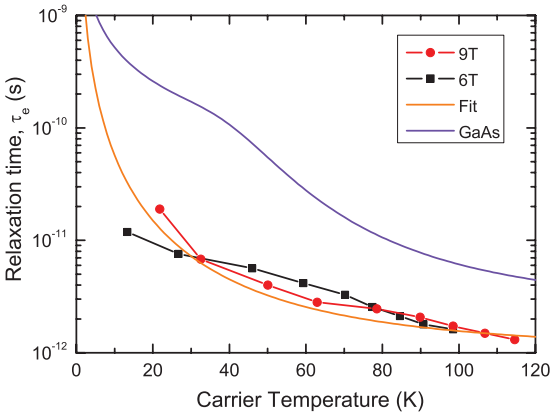


FIG. 5. (Color online) Relaxation time vs carrier temperature. A good fit is observed to the theoretical prediction, especially in the range of 30–80 K, which covers the regime of quantum Hall breakdown. A trace for GaAs[33] is shown by way of comparison. The GaAs has a relaxation time an order of magnitude slower than that of graphene across the entire temperature range.

surprising result that $\tau_e$ is typically an order of magnitude less than GaAs over the whole temperature range studied, resulting in a much higher energy loss rate in graphene. This is despite the fact that optic phonon emission is making a strong contribution to the GaAs energy loss rate above ∼50 K.

### B. Quantum Hall effect breakdown

To explore the potential of this system further as a resistance standard, we also examined the breakdown of the quantum Hall effect (QHE) at high currents. Figure 6 shows typical curves for two measurements of $V_{xx}$ at the resistivity minimum for $\nu = 6$. The appearance of a finite resistivity is used to predict the quantization accuracy, which is usually related to the Hall resistivity by $\Delta\rho_{xy} = -S\rho_{xx}$ where $S$ is a constant related to

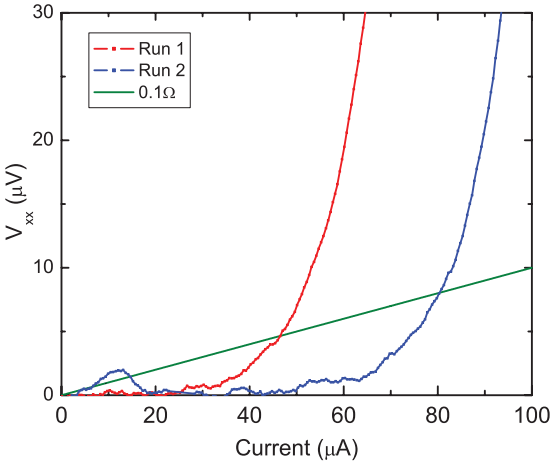


FIG. 6. (Color online) High current breakdown of $\nu = 6$ quantum Hall state in graphene. Defined as $R_{xx} < 0.1\ \Omega$ (green line), the breakdown current is 80 $\mu$A at 9.5 T for contacts 10 $\mu$m apart. Two successive runs are shown demonstrating the effect of current annealing on the breakdown behavior. This data was taken in the same configuration as the Shubnikov-de Haas data, with the current running from C to I.

the width of the probe arms over the width of the Hall bar, usually in the region 0.1–1.[34–36] The breakdown shows fairly typical behavior, with a relatively "soft" increase in resistance.

The sample exhibits the previously reported current annealing behavior[7,37] where the critical current increases as a result of passing a high current through the sample, probably due to the removal of physisorbed molecules which act as scattering centers. Using a fairly stringent definition[38] for the onset of breakdown at $R_{xx} = 0.1\ \Omega$ gives breakdown currents of ∼80 $\mu$A, flowing between contacts C and I in the inset to Fig. 1 corresponding to a peak current density of 10 $\mu$A/$\mu$m. This compares with previously reported[7,8] values of around 2–3 $\mu$A/$\mu$m at the considerably lower lattice temperature of 0.35 K for exfoliated graphene, and more recently values of around 10 $\mu$A/$\mu$m have been reported[9] in polymer gated epitaxial graphene.

We attribute this improvement over previous samples to two factors. Firstly, our improved contacting procedures, using gold without any adhesion layer for the region where the tracks contact the graphene. This gave an estimated contact resistance of 150–300 Ω $\mu$m from a comparison of two and four terminal measurements of the quantum Hall resistance on a similar sample using an identical contacting procedure. This compares very favorably to Ti/Au, Cr/Au, and Ni/Au which have typical contact resistances of $10^3$–$10^5$ Ω $\mu$m, and even compares favorably to Ti/Pd/Au which has a contact resistance of around 750 Ω $\mu$m.[39–43] Additionally we attribute the improvement to our use of an internal contacting geometry which minimizes scattering from defect edge states. These breakdown current values demonstrate that there is almost an order of magnitude increase over the largest values reported[10,44] for GaAs devices which are typically in the range 1–2 $\mu$A/$\mu$m.

The observation of enhanced breakdown currents in graphene is due to the combination of two favorable factors: the increased cyclotron energy combined with the larger energy loss rates measured above. This can be seen from the most commonly used model to predict the breakdown of QHE, which is the bootstrap-type electron heating model of Komiyama and Kawaguchi,[45] which is based on the runaway heating which occurs when the quantum Hall effect begins to break down. Modifying this theory for the two-fold valley degeneracy of graphene, the breakdown field $E_y$ is predicted to be

$$E_y = \sqrt{\frac{4B\hbar\omega_c}{\eta e\tau_e}}, \tag{10}$$

where $\eta = 4$ for graphene, to account for the two-fold spin and two-fold valley degeneracy.

The breakdown currents found above correspond to a carrier temperature of 50–70 K where it was found that $\tau_e \sim 3$ ps. This value is ∼30 times smaller than for GaAs, which suggests that breakdown currents will be much higher in graphene as a result of this. In fact Eq. (10) suggests that this factor will be more important than the increased value of $\hbar\omega_c$ for graphene. Using Eq. (10) we compare the predictions for graphene ($\nu = 2,6$) with GaAs ($\nu = 2$), the current gold standard for resistance metrology measurements, shown in Table I. The carrier densities are adjusted to correspond to each plateau occurring at 10 T. The bootstrap heating model

TABLE I. Data calculated for the cyclotron energy, carrier relaxation time, breakdown current per micrometer, and thermal breakdown temperature, with carrier densities set for each plateau such that the labeled plateaux all occurred at 10 T.

| At 10 T: | GaAs ($\nu = 2$) | Graphene ($\nu = 6$) | Graphene ($\nu = 2$) |
|---|---|---|---|
| $\hbar\omega_c$ (meV) | 17 | 51.6 | 126 |
| $\tau_e$ (ps) | 100 | 3 | 4 |
| $I_b = \nu\sigma_0 E_b$ ($\mu$A/$\mu$m) | 4.7 | 93 | 43 |
| $T$ (K) | 4 | 12 | 30 |

predicts that graphene should be 10–20 times better than GaAs, although the predicted values are significantly higher than those observed to date for both materials. In the experiments above, breakdown current densities approximately 5–10 times larger than those observed in good GaAs Hall bars were obtained, suggesting that further optimization might be able to increase the breakdown currents in graphene still further. It is also worth noting that for this device we did not attempt an extensive optimization of the annealing procedure, and in previous work[8] significant improvements in breakdown currents were observed when decreasing temperature from 1.5 to 0.35 K. The theory has thus allowed us to conclude that the majority of the improvement to the breakdown current in graphene is in fact due to its high energy loss rate associated with the small value of $\tau_e$.

A further advantage of graphene for metrology is that it could be used to allow such measurements to be carried out at much higher temperatures due to the higher cyclotron energies. In order to achieve the accuracy that standards require,[8] currently about one part in $10^{10}$, which corresponds to

$$\rho_{xx} \ll 10^{-10}\rho_{xy}, \tag{11}$$

where for high mobility samples

$$\rho_{xx} \approx \frac{1}{\nu\sigma_0}\exp\left(-\frac{\hbar\omega_c}{2k_BT}\right), \tag{12}$$

due to thermal excitations across the Landau gap. To get the required one part in $10^{10}$ accuracy, we need

$$k_BT < \hbar\omega_c/50. \tag{13}$$

Using this criterion we calculate the temperature at which thermal breakdown of the quantum Hall effect will occur. This is shown in Table I. As one can see, thermal breakdown of the quantum Hall effect should occur at much higher temperatures in graphene than in GaAs and crucially it should be possible to achieve standards level quantization at temperatures up to 10 K, in contrast to the 0.3 K typically used in GaAs standards measurements.

## IV. CONCLUSIONS

We have shown experimentally that electron energy loss in graphene follows the predictions of deformation potential coupling going as $\sim T^4$ at carrier temperatures up to $\sim$100 K. We have shown that this is in good agreement with deformation potential theory[5] when modified with a limiting relaxation time. From this we conclude that the energy relaxation time in graphene is over an order of magnitude shorter than that of GaAs.

As a result of the much shorter relaxation time in particular, we expect that QHE breakdown currents should be much higher in graphene when compared to GaAs. We have observed this using exfoliated graphene, and the prediction suggests that future improvements to sample preparation could allow for yet higher breakdown currents. High breakdown currents have been observed at Helium 4 temperatures, and estimates suggest that high breakdown currents should be observable at even higher temperatures which would allow for easier fabrication of cryogen-free metrology kits.

## ACKNOWLEDGMENTS

We thank the EPSRC for continued support for this work.

*r.nicholas1@physics.ox.ac.uk

[1] [http://www.itrs.net/links/2009ITRS/Home2009.htm], Semiconductor Industry Association 2009 (2009).
[2] K. S. Novoselov, Z. Jiang, Y. Zhang, S. V. Morozov, H. L. Stormer, U. Zeitler, J. C. Maan, G. S. Boebinger, P. Kim, and A. K. Geim, Science **315**, 1379 (2007).
[3] T. Palacios, Nature Nanotech. **6**, 464 (2011).
[4] F. Schwierz, Nature Nanotech. **5**, 487 (2010).
[5] S. S. Kubakaddi, Phys. Rev. B **79**, 075417 (2009).
[6] W.-K. Tse and S. Das Sarma, Phys. Rev. B **79**, 235406 (2009).
[7] A. J. M. Giesbers, G. Rietveld, E. Houtzager, U. Zeitler, R. Yang, K. S. Novoselov, A. K. Geim, and J. C. Maan, Appl. Phys. Lett. **93**, 222109 (2008).
[8] A. Tzalenchuk, S. Lara-Avila, A. Kalaboukhov, S. Paolillo, M. Syväjärvi, R. Yakimova, O. Kazakova, T. J. B. M. Janssen, V. Fal'ko, and S. Kubatkin, Nature Nanotech. **5**, 186 (2010).
[9] T. J. B. M. Janssen, A. Tzalenchuk, R. Yakimova, S. Kubatkin, S. Lara-Avila, S. Kopylov, and V. I. Fal'ko, Phys. Rev. B **83**, 233402 (2011).
[10] Y. Ma, R. Fletcher, E. Zaremba, M. D'Iorio, C. T. Foxon, and J. J. Harris, Phys. Rev. B **43**, 9033 (1991).
[11] D. Sun, Z.-K. Wu, C. Divin, X. Li, C. Berger, W. A. de Heer, P. N. First, and T. B. Norris, Phys. Rev. Lett. **101**, 157402 (2008).
[12] J. M. Dawlaty, S. Shivaraman, M. Chandrashekhar, F. Rana, and M. G. Spencer, Appl. Phys. Lett. **92**, 042116 (2008).
[13] M. Freitag, M. Steiner, Y. Martin, V. Perebeinos, Z. Chen, J. Tsang, and P. Avouris, Nano Lett. **9**, 1883 (2009).
[14] J.-H. Chen, C. Jang, S. Xiao, M. Ishigami, and M. S. Fuhrer, Nature Nanotech. **3**, 206 (2008).
[15] K. Bolotin, K. Sikes, Z. Jiang, M. Klima, G. Fudenberg, J. Hone, P. Kim, and H. Stormer, Solid State Commun. **146**, 351 (2008).

[16]K. S. Novoselov, A. K. Geim, S. V. Morozov, D. Jiang, Y. Zhang, S. V. Dubonos, I. V. Grigorieva, and A. A. Firsov, Science **306**, 666 (2004).
[17]P. Blake, E. W. Hill, A. H. Castro Neto, K. S. Novoselov, D. Jiang, R. Yang, T. J. Booth, and A. K. Geim, Appl. Phys. Lett. **91**, 063124 (2007).
[18]L. Liu, S. Ryu, M. R. Tomasik, E. Stolyarova, N. Jung, M. S. Hybertsen, M. L. Steigerwald, L. E. Brus, and G. W. Flynn, Nano Lett. **8**, 1965 (2008).
[19]W. J. Duffin, *Electricity and Magnetism* (W. J. Duffin Publishing, Cottingham, 2001).
[20]D. R. Leadley, R. J. Nicholas, J. J. Harris, and C. T. Foxon, Solid-State Electron. **32**, 1473 (1989).
[21]G. Stöger, G. Brunthaler, G. Bauer, K. Ismail, B. S. Meyerson, J. Lutz, and F. Kuchar, Phys. Rev. B **49**, 10417 (1994).
[22]D. R. Leadley, R. J. Nicholas, J. J. Harris, and C. T. Foxon, Semicond. Sci. Technol. **4**, 879 (1989).
[23]R. Leturcq, D. L'Hote, R. Tourbot, V. Senz, U. Gennser, T. Ihn, K. Ensslin, G. Dehlinger, and D. Grutzmacher, Europhysics Lett. **61**, 499 (2003).
[24]M. Breusing, C. Ropers, and T. Elsaesser, Phys. Rev. Lett. **102**, 086809 (2009).
[25]V. P. Gusynin and S. G. Sharapov, Phys. Rev. Lett. **95**, 146801 (2005).
[26]T. Ando, J. Phys. Soc. Jpn. **37**, 1233 (1974).
[27]R. S. Deacon, K. C. Chuang, R. J. Nicholas, K. S. Novoselov, and A. K. Geim, Phys. Rev. B **76**, 081406 (2007).
[28]U. Klass, W. Dietsche, K. Von Klitzing, and K. Ploog, Z. Phys. B **82**, 351 (1991).
[29]R. Fletcher, V. M. Pudalov, Y. Feng, M. Tsaousidou, and P. N. Butcher, Phys. Rev. B **56**, 12422 (1997).
[30]E. Chow, H. P. Wei, S. M. Girvin, and M. Shayegan, Phys. Rev. Lett. **77**, 1143 (1996).
[31]A. M. DaSilva, K. Zou, J. K. Jain, and J. Zhu, Phys. Rev. Lett. **104**, 236601 (2010).
[32]P. A. George, J. Strait, J. Dawlaty, S. Shivaraman, M. Chandrashekhar, F. Rana, and M. G. Spencer, Nano Lett. **8**, 4248 (2008).
[33]K. Leo, W. W. Ruhle, and K. Ploog, Phys. Rev. B **38**, 1947 (1988).
[34]F. Delahaye and B. Jeckelmann, Metrologia **40**, 217 (2003).
[35]M. Furlan, Phys. Rev. B **57**, 14818 (1998).
[36]B. Jeckelmann and B. Jeanneret, Rep. Prog. Phys. **64**, 1603 (2001).
[37]K. I. Bolotin, K. J. Sikes, J. Hone, H. L. Stormer, and P. Kim, Phys. Rev. Lett. **101**, 096802 (2008).
[38]G. Nachtwei, Physica E **4**, 79 (1999).
[39]B.-C. Huang, M. Zhang, Y. Wang, and J. Woo, Appl. Phys. Lett. **99**, 032107 (2011).
[40]P. Blake, R. Yang, S. V. Morozov, F. Schedin, L. A. Ponomarenko, A. A. Zhukov, R. R. Nair, I. V. Grigorieva, K. S. Novoselov, and A. K. Geim, Solid State Comm. **149**, 1068 (2009).
[41]S. Russo, M. F. Craciun, M. Yamamoto, A. F. Morpurgo, and S. Tarucha, Physica E **42**, 677 (2010).
[42]K. Nagashio, T. Nishimura, K. Kita, and A. Toriumi, Appl. Phys. Lett. **97**, 143514 (2010).
[43]K. Nagashio, T. Nishimura, K. Kita, and A. Toriumi, Jpn. J. Appl. Phys. **49**, 051304 (2010).
[44]S. Kawaji, K. Hirakawa, M. Nagata, T. Okamoto, T. Fukase, and T. Gotoh, J. Phys. Soc. Jpn. **63**, 2303 (1994).
[45]S. Komiyama and Y. Kawaguchi, Phys. Rev. B **61**, 2014 (2000).